damping to a small value, one which can be allowed for in interpreting the results.

It would be considerably more profitable, however, to retain the present form of the apparatus. The fact that no mechanical connection to the rotor is required provides certain advantages. It would be possible, for instance, to seal the rotor into a pressure chamber so as to make measurements at pressures above the vapor-pressure line; measurements could also be made in He^3, for example, by filling the chamber and sealing it at room temperature.

Note added in proof.—The question has arisen as to why we made no attempt to circumvent the difficulty of thermomechanical flow by making measurements above the λ point. This would have required the use of a double helium bath and radiation shielding to reduce convection flow to a tolerable level. Such extensive modifications of the apparatus seemed beyond the scope of the present work, which was intended to resolve some difficulties concerning the anomalous behavior of helium II. The viscosity of helium I has been measured satisfactorily by various other methods.

PHYSICAL REVIEW VOLUME 102, NUMBER 3 MAY 1, 1956

Photoconductivity in Manganese-Doped Germanium

R. NEWMAN, H. H. WOODBURY, AND W. W. TYLER
General Electric Research Laboratory, Schenectady, New York

(Received December 12, 1955)

Impurity photoconduction has been observed in *n*- and *p*-type Mn-doped germanium at low temperatures. The spectra are consistent with the published ionization energy values determined from conductivity data High-resistivity *n*-type samples show high intrinsic photosensitivity and long response times at low temperatures. In such samples the intrinsic photocurrent could be quenched by a factor of $\sim 10^4$ with light in the 0.3 to 0.7 ev range. Intrinsic photoconductivity was found to vary more rapidly than linearly with light intensity over a limited range.

INTRODUCTION

A PREVIOUS publication has described some of the electrical properties of Mn-doped germanium.[1] In this paper we shall describe some of the electro-optical properties with particular reference to photoconductivity. In earlier papers[2–7] measurements of the photoconductivity spectra, photoconductive yield, quenching of photoconductivity, and optical absorption of injected carriers for germanium doped with the elements Au, Fe, Ni, and Co have been reported. The behavior of Mn-doped germanium is qualitatively similar to these other cases. However, a number of the effects which were just barely measurable for the other materials are quite pronounced and readily measurable for Mn-doped germanium. For this reason a somewhat extended report of this work is presented.

EXPERIMENTAL

The method of crystal preparation has been described in earlier publications as have the details of the optical measurements.[1–7]

RESULTS AND DISCUSSION

A. Photoconductive Spectra

It has been found that Mn introduces two acceptor centers in germanium, one located 0.37 ev below the conduction band (upper level) and one located 0.16 ev above the valence band (lower level).[1] By suitable control of the ratio of ordinary donors and Mn acceptors, samples can be prepared for which the Fermi level is "locked-in" at either one level or the other at low temperatures.[1] In Fig. 1 are shown typical photoconductive spectra for *n*- and *p*-type samples of Mn-doped germanium for which the Fermi level is "locked-in" at the upper and lower Mn levels, respectively. These spectra can be divided into two regions in the usual way. At photon energies in excess of about 0.7 ev the response is due to intrinsic photoconductivity. Below about 0.7 ev the response is impurity photoconductivity which presumably results from the photoexcitation of carriers from the Mn centers.[6] The shapes of the two curves of impurity response in Fig. 1 are similar to those found for other double acceptor impurities. The impurity response for *p*-type samples shows a more or less flat plateau terminated at the low-energy side by a sharp drop in response at an energy approximately that found by electrical-conductivity methods. The *n*-type samples show no well-defined low-energy threshold but rather a monotonic decrease

[1] H. H. Woodbury and W. W. Tyler, Phys. Rev. **100**, 659 (1955).
[2] R. Newman, Phys. Rev. **94**, 278 (1954).
[3] R. Newman and W. W. Tyler, Phys. Rev. **96**, 882 (1954); W. W. Tyler and H. H. Woodbury, Phys. Rev. **96**, 874 (1954).
[4] Tyler, Newman, and Woodbury, Phys. Rev. **97**, 669 (1955).
[5] Tyler, Newman, and Woodbury, Phys. Rev. **98**, 461 (1955).
[6] W. W. Tyler and R. Newman, Phys. Rev. **98**, 961 (1955).
[7] R. Newman, Phys. Rev. **96**, 1188 (1954).

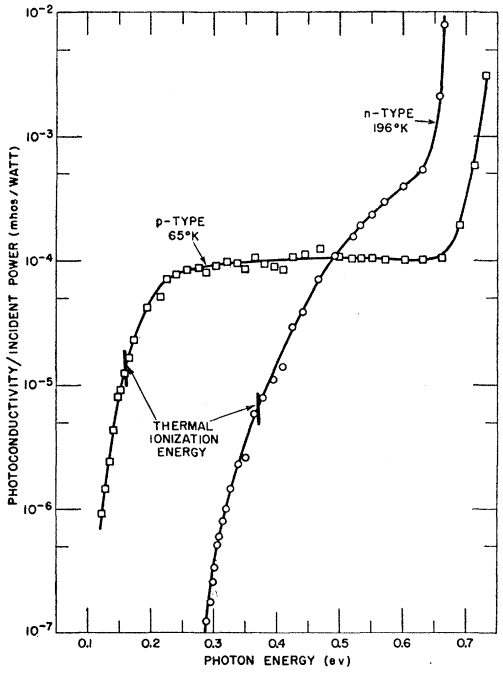

FIG. 1. Photoconductive spectra of n- and p-type Mn-doped germanium.

in response toward lower energies terminated by a region of very rapidly decreasing response.[8]

M. H. Hebb has suggested a possible mechanism to explain the difference between the shapes of the n- and p-type response curves. Assuming that the double-acceptor model of the Mn centers is correct, then the photoionization of a hole in p-type material will occur from a neutral Mn center and the photoionization of an electron in n-type material will occur from a doubly negative Mn center. In the latter case there will be a potential hill for electrons separating the bound state of the Mn and the bottom of the conduction band. H. Ehrenreich of this laboratory has shown, using a simple model for the potential, that for transitions to states near the bottom of the conduction band the transition probability increases more rapidly with increasing energy with the potential hill present than without it. This is in the direction suggested by the photoconductivity curves.

B. Intrinsic Photoconductivity

Previous work has shown that the presence of double-acceptor impurities in germanium controls the lifetime of injected carriers. Of particular interest was the fact that at low temperatures hole traps are produced by the presence of these elements. The effect of these traps is most clearly shown in n-type material. The low-temperature trapping effects and the room-temperature recombination effects were shown to be explicable on the basis of the double-acceptor model.[3]

Figure 2 shows a plot of steady-state photocurrent *vs* reciprocal temperature for a high-resistance sample whose dark current over the range of temperature shown was less than 1 μA for $1\frac{1}{2}$ volts applied. Curves for two different incident light intensities are shown. The curves of Fig. 2 show a region of exponential behavior for the photocurrent which presumably reflects the exponential dependence of the photoconductive time constant. The slope is roughly 0.3 ev.

The data of Fig. 2 show a plateau at low temperatures. One can assume that in the exponential region that the photoconductive time constant is determined by some thermal activation process (e.g., evaporation from hole traps). In the region of the plateau this is no longer the limiting factor but rather the time constant is presumably determined by some temperature independent process. It is worth noting that in several low-resistance n-type Mn-doped crystals, curves of the photoconductive decay times *vs* reciprocal temperature showed a qualitative similarity to the curves of Fig. 2.[9] That is, there was shown to be an exponential region with a slope of about 0.3 and a plateau at low temperatures.

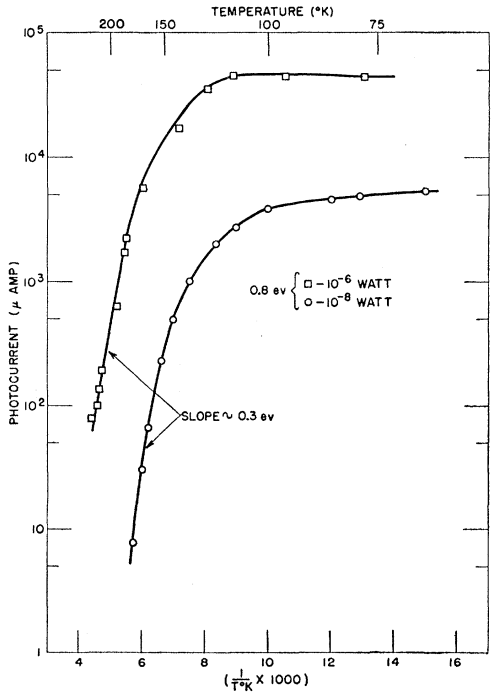

FIG. 2. Intrinsic photocurrent *vs* reciprocal temperature for a high-resistivity n-type Mn-doped crystal, $h\nu = 0.8$ ev, 1.5 v applied. The effect is shown for two light levels.

[8] It is of interest to note that samples were obtained which had impurity response curves that seemed to result from a superposition of the n- and p-type response curves. These samples were p-type. However, for these, the estimated fraction of the lower Mn level occupied by electrons was close to unity. It is not certain whether the photoconductive spectra for these intermediate cases resulted from local inhomogeneities (i.e., p and n regions) too small to measure by probing techniques or were truly a property of a homogeneous crystal.

[9] W. W. Tyler and H. H. Woodbury, Bull. Am. Phys. Soc. 1 (Series II, No. 3), 127 (1956).

Figure 3 shows a log-log plot of the steady-state intrinsic photoconductivity for a high-resistance n-type Mn-doped crystal as a function of incident light intensity at a photon energy of 0.8 ev[10] for several temperatures. Of particular interest is the fact that regions are shown where the photocurrent varies with a power of the light intensity different from unity.[11] For future use we will designate this power by α. This type of behavior was shown by the three n-type Mn-doped samples that were studied. At each of the temperatures for which data are given, there is a range for which $\alpha>1$ at low light levels which goes over into a range for which $\alpha<1$ at higher light levels. The maximum value of α decreases with increasing temperature, ranging from about 3.5 at 77°K to 1.4 at 140°K.

In order to ascertain whether the intensity dependence was in any way an effect due to the applied field (e.g., injection), the photocurrent *vs* intensity was measured for a series of applied voltages ranging from 0.1 v to 22 v. No pronounced effect was found. Although the photocurrent for a given light intensity was not strictly linear with applied voltage, particularly below 1 volt, the different photocurrent *vs* light intensity curves for the various voltages were essentially identical except for the voltage-dependent scaling factors.

At several of the data points of Fig. 3 we have indicated some time-constant data. The times designated

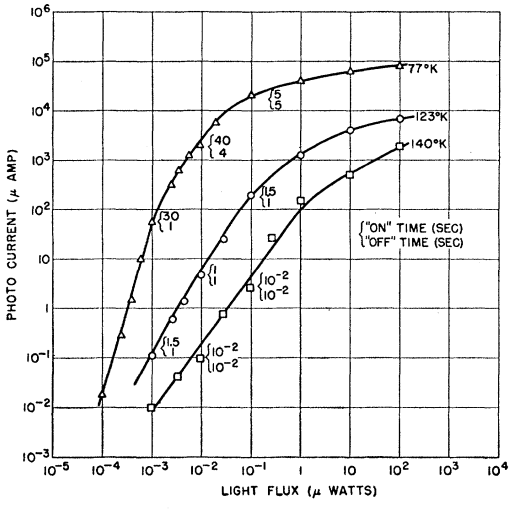

FIG. 3. Intrinsic photocurrent in an n-type high-resistivity sample *vs* light flux ($h\nu=0.8$ ev) at several temperatures. $22\frac{1}{2}$ v applied.

[10] Data taken at other photon energies were equivalent. This particular value was chosen because the penetration depth for the light was about the sample thickness.

[11] In order to exclude geometric effects, measurements in this range were taken with a fixed monochromator slit width. The slit image was parallel to the direction of current flow and extended with essentially uniform brightness the entire length of the sample. The attenuation of the beam was achieved by interposing a series of neutral filters (e.g., diaphragms and/or wire mesh). In practice it turned out that the photocurrents were almost independent of the method of obtaining a given flux on the sample so that the technique using neutral filters was an unnecessary refinement.

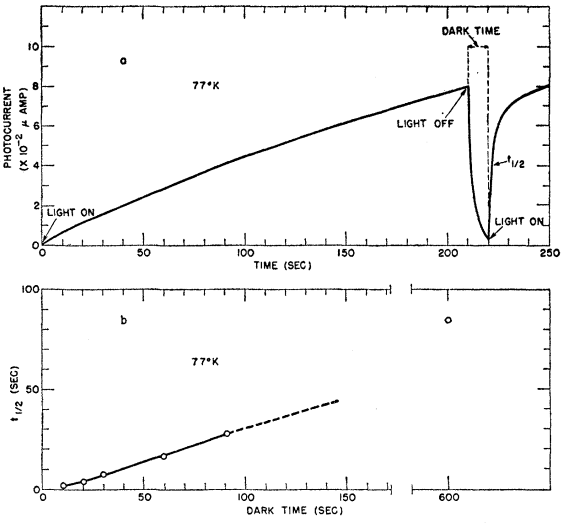

FIG. 4. Intrinsic photocurrent in an n-type high-resistivity sample ($h\nu=0.8$ ev) as a function of illumination history (see text) at 77°K.

as "on" represent the time required to reach $\frac{1}{2}$ the ultimate photocurrent from the dark value. Those designated "off" represent the time required for the photocurrent to decay to $\frac{1}{2}$ its steady state value. Since the transient response is not simply exponential, the times are not of themselves too significant but do indicate orders of magnitude.

A measurement was also made of the intensity dependence of the impurity photoconductivity in the same n-type crystal from which the data of Fig. 3 were obtained. The measurement was made at 77°K at an incident photon energy of 0.60 ev. This dependence was almost linear over the two lowest decades of response. The measured slope on a log-log plot was 1.2. This is in contrast to the case for intrinsic photoconductivity where at 77°K the measured slope was about 3.5 over the same range of photocurrent.

The high-resistivity n-type crystals showed an interesting memory effect. Namely, the shape of the photoconductivity *vs* time curve under constant illumination was a function of how long the sample had previously been maintained in the dark. Figure 4(a) shows the data of a cycle of events which shows the effect most clearly. The decay curves in the dark were all identical, independent of previous history. Figure 4(b) is a plot of an effective photoconductive risetime ($t_{\frac{1}{2}}$) against the time in the dark for a sample at 77°K. At the particular light level used ($\sim 2\times10^{-9}$ watt, $h\nu=0.8$ ev,) the sample was in the range for which $\alpha>1$. At higher light levels the memory effect was less pronounced. In the range for which $\alpha<1$ it was not observed.

C. Quenching of Intrinsic Photoconductivity

In the earlier work on doping with double acceptors it was found that there was a correspondence between the existence of high intrinsic photosensitivity in n-type

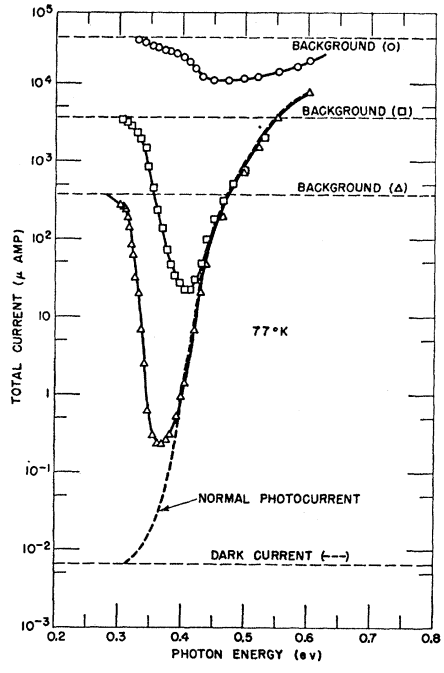

FIG. 5. Quenching spectrum of an n-type high-resistivity sample at 77°K. The effect of different background light levels is shown (see text).

material and the quenching of this photosensitivity by infrared light with photon energies somewhere in the extrinsic range. This quenching effect has been explained as follows:

1. Intrinsic excitation produces free electrons and trapped holes.

2. The recombination of the electrons and the trapped holes is slow so that a large electron population is built up.

3. Infrared quenching light excites the holes to a configuration in which the recombination between the electrons and the excited holes is faster than as in (2).

4. The faster recombination lowers the steady-state electron population and the photocurrent is quenched.

In the n-type high-photosensitivity Mn-doped samples a quenching effect, larger than any previously reported, has been found. Under a particular set of conditions it was possible to reduce the photocurrent by almost a factor of 10^4 as shown in Fig. 5.

In making these measurements the sample is first illuminated with a light source termed the background light (a tungsten lamp in the present case) whose chief effect is to produce intrinsic photoconductivity. The total current thus produced for a particular background light intensity is termed the background current and is designated on Fig. 5 by a horizontal dashed line. By varying the background light flux on the sample, different background currents can be achieved. Keeping the background light flux a constant, the sample is then simultaneously illuminated with monochromatic light of the desired wavelength and the total current thus produced at steady state is observed. This current is the ordinate of Fig. 5. If the total current under these conditions is less than the background current then the latter is said to be quenched.

We should like to note again that the effect is independent of the method of producing the intrinsic photoconductivity. The effect may be obtained even when *all* light incident upon the sample passes through a germanium filter kept at room temperature. This last observation would seem to indicate that a true bulk effect is being observed and not some surface phenomenon.

Figure 5 shows the effect of the monochromatic beam at several different background light values including one labeled "dark current" for which the all intentional background light was eliminated. The monochromatic light intensity was a constant at any given wavelength for all the curves. Over the range from 0.6 ev to 0.3 ev the power in the monochromatic beam incident on the sample decreased less than a factor of three which means an almost constant number of incident quanta at each wavelength over this range. No attempt has been made to correct the curves of Fig. 5 for this small variation.

The curve marked "normal photocurrent" is the response curve for the sample without any intentional background light. It is, with appropriate normalization, the same as the n-type impurity response shown in Fig. 1. One can assume to first approximation that this impurity photoconductivity can be simply subtracted from the total current to give a current whose spectral dependence will more precisely reflect the quenching effect than will the total current. If this subtraction procedure is valid one finds that the quenching spectrum has a peak at about 0.4 ev with a sharp low-energy

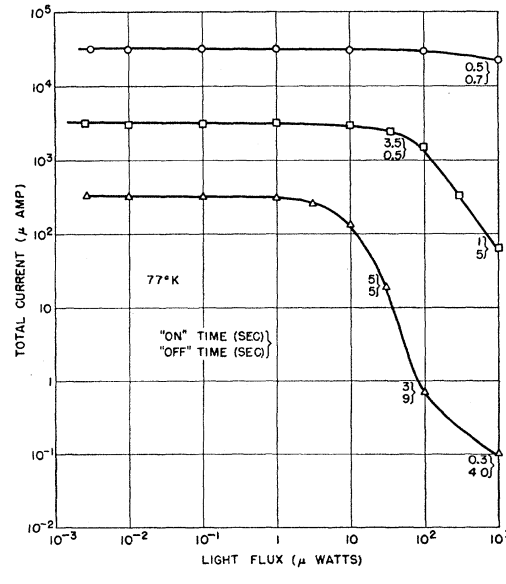

FIG. 6. The quenching effect at 77°K as a function of quench light flux. The effect at different background light levels is shown.

threshold somewhere in the range 0.30–0.35 ev and a slowly decreasing high-energy tail extending to energies higher than 0.6 ev. This can be understood in terms of an excitation of the hole from its trapped configuration to the continuum.

In Fig. 6 are shown some log-log plots of the total current as a function of the flux of monochromatic quenching light (0.4 ev) incident on the sample at 77°K. The effect on several background photocurrents is shown. On this figure we have also indicated at various data points some of the time constants characterizing the quenching process.

The designation "on" in Fig. 6 refers to the time required for the background current to decay to half its initial value after the quenching light is turned on. The designation "off" refers to the time required for the background current to reach half its final value after the quench light is turned off. Again these times are only included to establish orders of magnitude. The curves are not of a simple exponential form.

We shall mention only briefly some results on the temperature dependence of the quenching effect. In the 77°K to 140°K range, the spectral dependence remains essentially unchanged. Measurements were made holding the background photocurrent constant at the different temperatures. Under those conditions it was found that the quench effect at a constant quench light flux decreased with increasing temperature. At the wavelength of maximum effect, typical factors by which the background current was reduced were 2×10^3 at 77°K, 2×10^2 at 120°K, and 3 at 140°K. Thus there is a qualitative correspondence between the temperature dependence of the quenching efficiency and intrinsic photosensitivity (e.g., see Fig. 2).

D. Injection Breakdown

Tyler[8] has shown that the phenomenon of injection breakdown was exhibited at 77°K by *n*-type high resistivity Fe-doped germanium. He reported the observation of one of the present authors (R. N.) that the breakdown could be quenched by illuminating the diode within the 0.3 ev–0.6 ev range. This could occur, however, only if the operating voltage was slightly greater than the minimum sustaining voltage in the dark. In the case of Mn-doped material this restriction on the operating voltage can be greatly relaxed. For example, for a unit which could be broken down in the dark at an applied voltage of ~50 volts and which could be maintained in the breakdown state at voltages greater than about one volt, it was possible to quench the breakdown using 0.4-ev light with an applied voltage as high as 15 volts. This greater voltage latitude presumably results from the greater efficiency for the quenching process in the Mn-doped germanium.

E. Absorption Due to Injected Carriers

We have measured the absorption spectrum of injected carriers in a breakdown diode of *n*-type Mn-doped germanium. It is found to be anomalous in the sense used in reference 7. The curve resembled that of curve *b*, Fig. 3, in that paper. That is, instead of a spectrum resembling that of free holes, a more or less flat structureless absorption obtained. Anomalous behavior was ascribed in reference 7 to the presence of hole traps. This is consistent with the observation of an anomalous spectrum for Mn-doped germanium.

CONCLUSIONS

The impurity photoconductive spectra of Mn-doped germanium are similar to those found for crystals doped with Au, Fe, Ni, and Co and support the energy level scheme developed from electrical conductivity data.[1]

The intrinsic photoconductivity in *n*-type crystals is complex. Although it is possible to explain qualitatively high photoyield, long response times, and quenching on the basis of the hole traps produced at doubly charged Mn centers, this does not appear to give a complete explanation. In particular it would not appear possible to explain the $\alpha>1$ behavior and memory effects with this simple picture.

A process which increases the lifetime with increase in the photoinjection level can give rise to an $\alpha>1$. Rittner[12] has shown how this can result from a single recombination level model for intrinsic photoconductivity. Rose[13] has suggested a two-level scheme that could also explain it. In Rose's model one of the levels would act as a recombination center, the other as a trapping center. To obtain an $\alpha>1$ the number of active recombination centers is decreased as the photoinjection level is increased.

Rose's picture possibly can be applied to the present case. The $\alpha>1$ and memory effects appear confined to carrier densities less than about $10^{11}/cm^3$ in contrast to the Mn concentration of about $10^{15}/cm^3$. In germanium there are usually recombination centers present in concentrations of the order of 10^{11}–$10^{12}/cm^3$.[14] Thus from consideration of orders of magnitude it would seem possible that the photoeffects that are being observed could involve both the added Mn and the unintentionally introduced recombination centers. For example, a specific recombination center might be a Ni, Co, or Fe atom. The energy of the recombination level for any of these ($E_r-E_c\sim0.3$ ev) relative to the equilibrium Fermi level ($E_f-E_c=0.37$ ev) would be proper for an application of Rose's model. This suggests the possibility that double-doping experiments (e.g., Mn+Ni, etc.) under proper control may provide a test of the applicability of Rose's model to the present case and give further insight into the mechanism of intrinsic photoconductivity.

[12] E. S. Ritter, Atlantic City Photoconductivity Conference (unpublished).
[13] A. Rose, Phys. Rev. **97**, 322 (1955).
[14] Burton, Hull, Morin, and Severiens, J. Phys. Chem. **57**, 853 (1953).